Metrology for the Advancementof X-ray Optics at the ALS

KENNETH A. GOLDBERG,[1] VALERIY V. YASHCHUK,[2] NIKOLAY A. ARTEMIEV,[2] RICHARD CELESTRE,[2] WEILUN CHAO,[1] ERIC M. GULLIKSON,[1] IAN LACEY,[2] WAYNE R. MCKINNEY,[2] DANIEL MERTHE,[2] HOWARD A. PADMORE[2]

[1]Center for X-ray Optics, Lawrence Berkeley National Laboratory, Berkeley, California, USA [2]Advanced Light Source, Lawrence Berkeley National Laboratory, Berkeley, California, USA

When it comes to building short-wavelength optical systems to control light at the nano-scale, metrology is the foundation, and accuracy is the bedrock. An inescapable truth in our field is that the most highly specified optical elements are wildly aberrated when just slightly misaligned, whether that misalignment comes from surface-figure or mirror-placement errors, imperfect bending, thermal drift, vibration, or other various anomalies.

It could be argued that recent advances in source brightness at upgraded synchrotrons and free-electron lasers have far outpaced improvements in the quality of X-ray optics and the beamlines that house them. A tour of the existing beamlines at many synchrotron facilities would reveal as much. Yet the demand for diffraction-limited performance, nano-focusing, and coherent wavefront control has led to a growing number of projects that aim to counter that imbalance. Investment in the performance of beamlines—with high-quality optics, strategic feedback, and improved engineering—has a high potential return relative to its cost, and to the cost of source updates. Honing the quality and reliability of beamline optics through improvements in metrology and feedback requires an integrated strategy at the convergence of several techniques. It comes with the promise of unlocking greater performance from imperfect mirrors.

Current research efforts in metrology at Lawrence Berkeley National Laboratory's (LBNL) Advanced Light Source (ALS) span a diverse range of applications, wavelengths, and target outcomes. We believe that integrating multiple techniques has enabled greater improvements than isolated measurements and applications could have produced individually. Advances in ex-situ visible-light optical metrology have led to a deeper understanding of the mirror-mounting and environmental requirements for bendable optics and to engineering improvements based on empirical tests. At-wavelength testing, using both coherent and incoherent techniques, has demonstrated rapid alignment feedback and sensitivity at diffraction-limited quality. Reflectometry continues its function as a cornerstone technique for investigations of coatings, surface quality, and materials properties. Nanofabrication plays a key role in the creation of calibrated elements for diffractive optics, interferometry, and as reference structures for quantifying the resolution of imaging techniques.

On tilts, slopes and curvatures

The center of gravity of ex-situ (in-lab) metrology at the ALS is shifting. The X-ray Optics Laboratory (XROL), a unique lab that serves the needs of several West Coast DOE research organizations, is currently moving to new facilities that promise improved conditions for measurement error minimization. The XROL serves several DOE labs

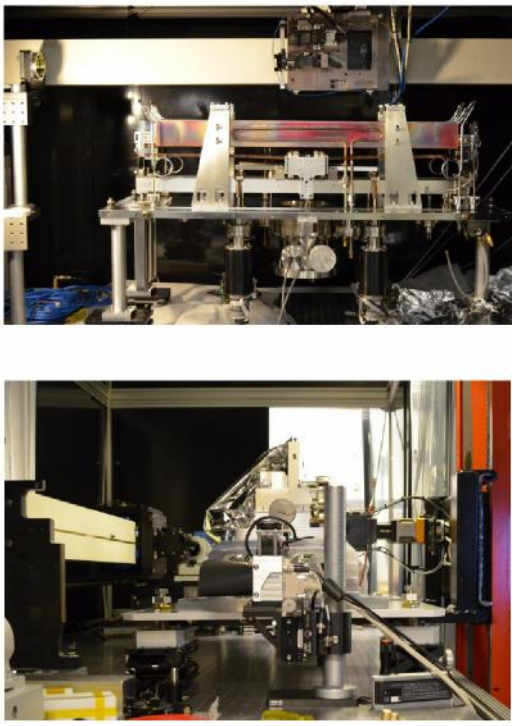

Figure 1: (a) The upgraded LTP-II [1] with a focusing mirror placed for best tuning to the desired longitudinal ellipse. A vertically adjustable gantry system of the LTP-II allows the instrument to accommodate mirror assemblies of different sizes. (b) The ALS DLTP [2] set up for optimal shaping of a bendable X-ray mirror designed for readjustment for two focal distances. The DLTP was recently modified for optimal measurement performance with side-facing optics.

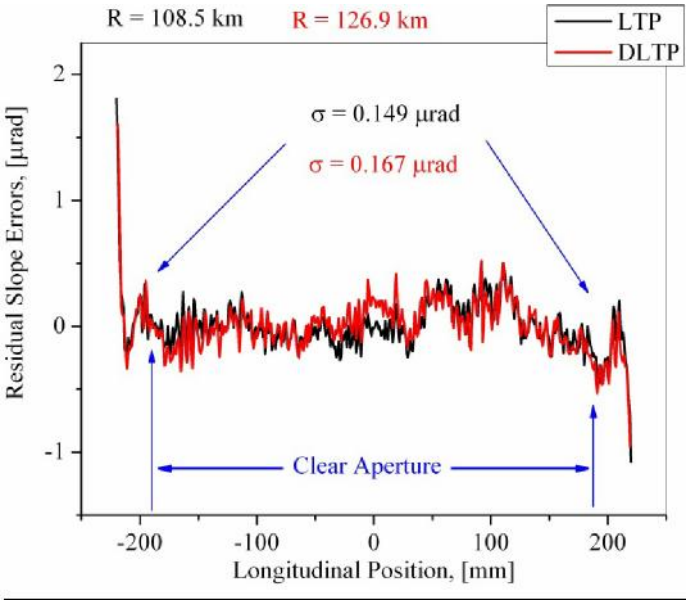

Figure 2: Cross comparison of the LTP and DLTP measurements with a flat mirror substrate. The cross comparison of measurements with principally different slope profilers, LTP-II and DLTP, enables a reliable estimation of the instrumental performance.

that lack dedicated on-site optical metrology capabilities, including the Linac Coherent Light Source (LCLS) at SLAC and the LBNL's Center for X-ray Optics (CXRO).

The major role of XROL is to proactively support the development and optimal beamline use of X-ray optics. On the beamline, combinations of imperfections interfere to degrade performance. Ex-situ metrology can characterize, analyze and, where possible, correct imperfections using laboratory tools and methods

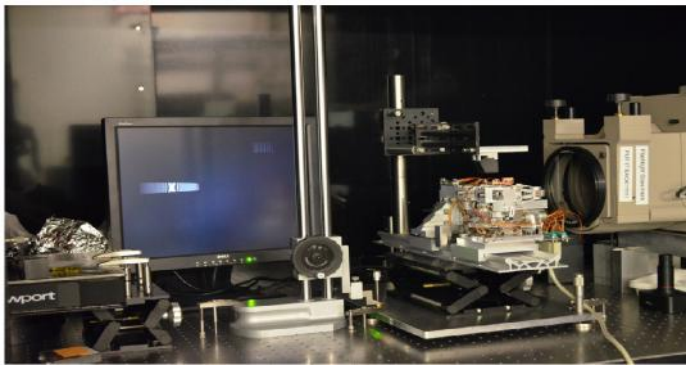

Figure 3: An example of the 6-in ZYGO™ GPI interferometer available at the ALS XROL used for the mutually orthogonal alignment of two small, bendable mirrors [13] for use in Kirkpatrick-Baez (KB) configuration. The vertically deflecting mirror (background) and the horizontally deflecting mirror (foreground) are mounted on a support rail identical to the beam-line arrangement. The respective interference fringes are displayed on the interferometer's monitor. The reflection from the upward-facing surface is viewed through a high-quality pentaprism.

independent of valuable beamtime.

For example, the long trace profilers available at the ALS XROL, the upgraded classical LTP-II [1] and the autocollimator-based Developmental LTP (DLTP) [2] (Figures 1a and 1b, respectively), provide a convenient way to set mirror adjustments before mirrors are put in a beamline. These slope profilers are used to assess mechanical mounting, bending, vibration, and cooling on the overall performance of optical elements. For characterization and tuning of mirror benders, original experimental procedures have been developed [3–5] that allow us to dramatically increase the precision and efficiency of surface slope metrology with bendable optics.

The accuracy of surface slope measurements demonstrated with the ALS slope profilers is below 60 nrad (rms) when measuring flat and close to flat optics (Figure 2). For significantly curved optics, it is approximately 250 nrad (rms). The accuracy is comparable to that of the world's best instruments at synchrotron metrology labs, such as the HZB/BESSY NOM [6-8] and SPring-8 LTP [9]. This is in spite of the fact that, in the current location, the ALS XROL slope profilers are compromised by poor environmental conditions that lead to 2–3 times higher level of random errors and about 10 times larger temporal fluctuations due to instrumental drifts. The state-of-the-art accuracy at the ALS XROL comes at the expense of extended data acquisition times, including original methods for the suppression of systematic and drift errors [10-11].

Similar to other slope profilers, the current performance of the LTPII and the DLTP is limited by systematic errors that are increased when the entire angular range is used, which occurs with significantly curved X-ray optics. The profiler's systematic errors will be reduced with a sophisticated calibration method suggested at the OML and based on a Universal Test Mirror (UTM) [12]. Work to develop a UTM system is in progress as a collaborative project of the ALS, HZB/BESSY-11, and PTB (Germany) metrology teams.

Interferometric testing is one of the most commonly used techniques in optical metrology due to its high resolution and sensitivity. Large field-of-view Fizeau interferometers are general metrology tools for 2D surface shape characterization in the height domain. In the ALS XROL, we have a rather old 6-in ZYGOTM GP1 interferometer that is extremely useful for controlling optical assembly processes and for setting precise mutual alignment of optical components (Figure 3).

At the ALS XROL, we have two interferometric optical microscopes, the MicroMapTM-570 and the ZYGOTM NewView-7300. The interferometric microscopes are our basic metrology tools for high-accuracy testing of the surface finish of X-ray optics with sub-Angstrom rms roughness measured over the mid-spatial wavelength region from about 1 μm to 5 mm. The standard list of output parameters of a microscope measurement includes values of roughness (residual slope) averaged over an area, or along a sample line. These values are limited by the bandwidth of the measuring instrument, rather than by the bandwidth required by the particular application. These parameters generally do not provide a sufficient description of the surface that can then be used for local finish polishing or for evaluation of the performance of the optic in modern X-ray beamline applications where diffraction- limited focusing and coherence preservation are desired.

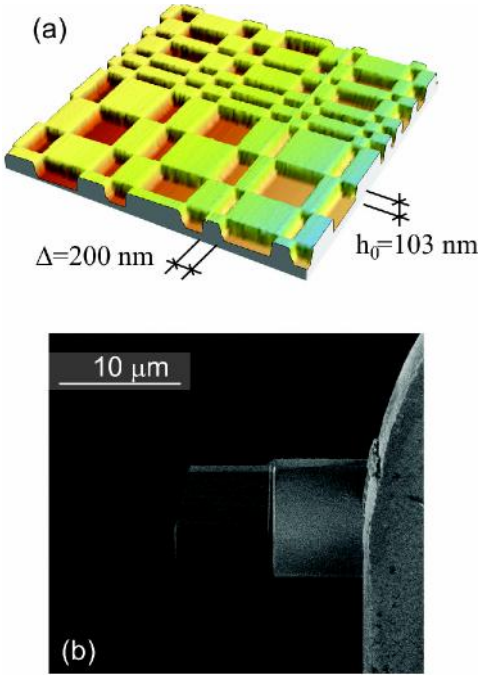

Figure 4: Examples of BPR test samples: (a) A scanning electron microscopy (SEM) image of a portion of a 2D array used for MTF calibration of interferometric microscopes [17]; (b) SEM image of the BPR multilayer test sample prepared using the FIB/SEM process and used for MTF calibration of electron scanning and transmission microscopes [18, 19] and, recently, for an X-ray microscope at the ALS.

In some cases (for example, X-ray scattering calculations, ex-situ metrology of X-ray diffraction gratings [14]), rigorous information about the expected performance of the optic can be obtained from a statistical description of the surface topography. The description is based on power spectral density (PSD) distributions of the surface height (or slope). Spectral analysis of the surface measurements is also used to parameterize, specify, and model the surface topography of optical components [15], as well as fabrication technologies, including optical polishing, lithography, surface coating, and multilayer deposition.

In order to account for the distortion effect of the instrumental modulation transfer function (MTF) on the PSD measurements, we have developed an MTF calibration method suitable for characterization of a broad class of surface profilometers [16-20]. The method is based on the use of binary pseudo-random (BPR) one-dimensional (2D) gratings and two-dimensional (2D) arrays as standard MTF test surfaces. Over a specific band of frequencies, the BPR distribution of two normalized physical levels/quantities (heights, materials, etc.) contains all frequencies in an equal amount. Unlike most conventional test surfaces, the inherent PSD of the BPR gratings and arrays has a white-noise-like character. Two examples of the calibration samples are depicted in Figure 4.

While appearing random, the array is constructed according to a strict mathematical formulation, and is explicitly determined. This allows the direct determination of the 1D and 2D MTFs, respectively, with a sensitivity uniform over the entire spatial frequency range of a profiler. Corresponding test objects based on binary pseudo-random distributions satisfy the requirements of a certified standard: functionality, ease of specification, reproducibility, and stability with respect to fabrication imperfections [20].

The scanning probe (atomic) microscope (SPM) Dimension-3100 is the main instrumental modality at the

ALS XROL for imaging at the nanoscale at high spatial frequencies, 10-10^6 mm^{-1}, corresponding to a wavelength range of -100 gm to -10 nm. High performance of the instrument is characterized by its sensitivity of about 0.1 nm to surface height variation. The instrument is used intensively for a project on the development of super-high-density X-ray diffraction gratings [21–24].

The ALS XROL is also equipped with a broad spectrum of optical instruments, such as a differential laser Doppler vibrometer and distance measuring interferometers, which are useful for the testing and characterization of opto-mechanical assemblies and components.

Concluding the description of capabilities for ex-situ metrology at the ALS, we should note that construction of a new optics lab, with comprehensive control of environmental conditions and clean-room 10,000 arrangements, is scheduled to be completed in late summer of 2013. After the move to the new lab is complete, and successive upgrades of the metrology tools are carried out, we expect significant improvement of all aspects of ex-situ metrology at the ALS.

Wavefront control and feedback: Mirrors getting in shape

Wavefront control and nano-focusing now drive progress in short-wavelength optical tools for science. For any such system, feedback is key. Like many aspheric focusing elements, KB mirrors tasked to perform at or near their resolution limit have small fields of view and are remarkably intolerant to misalignment, including simple displacements that shift the conjugate positions. Following ex-situ, visible-light shape optimization, final alignment on the beamline provides an opportunity to refine all of the degrees of freedom and measure the experimental sensitivities, provided that the available feedback is up to the task.

One project at the ALS created a soft X-ray focusing-mirror test-bed where different alignment and wavefront-sensing approaches could be developed and compared side by side [25-27] (Figure 5). This work traces its origins to interferometry conducted on EUV optical elements designed as research prototypes for photolithography at 13.5-nm wavelength. Those tests pushed numerical aperture values up to 0.3-NA,

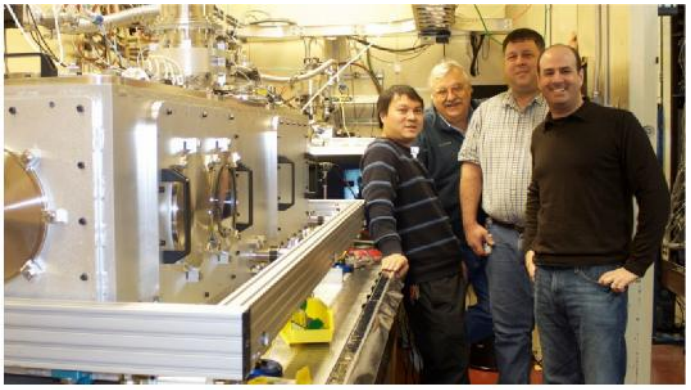

Figure 5: Experimental set-up at the ALS beamline 5.3.1 for testing of at-wavelength metrology for optimal in-situ alignment and tuning of bendable KB mirrors. Diffraction-limited focusing of soft X-rays (~1 keV) has been achieved [26].

where the difficulty increases substantially due to geometric systematic errors.

The goal was to reach diffraction-limited focusing, with mirror-slope sensing and control with feedback, below 100-nrad. Integration with visible-light mirror-shape optimization provided a solid head start for work performed on the beamline, and important feedback for test sensitivities.

The project focused on a pair of 100-mm-long KB mirrors scavenged from other projects and repurposed for this 2-D focusing application. Relatively short focal lengths (120 and 245 mm) and modest magnification ratios of 13 and 6, respectively, allowed the components to fit within a dedicated, 2-m-long, vibration-isolated test chamber.

A single optical rail connected to an internal breadboard provided a shared, stable platform for several critical components. The breadboard was coupled through bellows in the chamber walls to an optical bench that spanned the length of the chamber. At the upstream conjugate position, an *xy* stage with an array of slits and pinholes (used one at a time) provided a spatially filtered, stable, coherent illuminating beam. The array enabled in-situ selection of the object with the optimal size. (Selection involved a trade-off between diffraction angle and flux.) Two independent mounts with five degrees of bending, tilting, and translation freedom

supported the two KB test mirrors. Earlier work demonstrated the importance of temperature stability for bent mirror mounts [13], so Peltier coolers were attached to the in-vacuum mounts to maintain constant temperature (Figure 6). In the focal plane, an array of beam sensing and probing tools was mounted to an *xyz* stage, in such a manner than they could be inserted and removed completely from the beam to perform various tests. Finally, an X-ray CCD camera was mounted 1.5 m downstream of focus, positioned to catch the entire output beam.

This great attention to thermal and vibration stability was born of difficult experiences on unstable beamlines elsewhere. We suspect that the fine-focusing ability of many beamlines is ultimately limited by vibration and drift of components upstream of the sample plane.

In this configuration, we were able to perform a variety of tests, in increasing order of sensitivity, for learning and cross-comparison. This experience revealed the relative merits of each technique. The sequence of measurements is briefly described here.

1. **First alignment.** Using a low-magnification in-vacuum visible- light microscope with a YAG scintillator crystal, the beam size and position could be measured near the focal plane. The microscope could be positioned downstream of focus during the initial set-up of the mirrors in vacuum to guarantee that the beam falls on the centers of the two mirrors.
2. **Star test.** Simply observing the appearance of the beam on the YAG microscope can reveal qualitative information about various dependencies and large aberrations, such as astigmatism (observed by moving through focus) and coma tails. It may often be the case that the resolution of the YAG-microscope system is limited to several times larger than the diffraction-limited KB focus at-wavelength. In such situations, more sensitive tests are required.
3. **Star test and scanning-slit test.** With the YAG-microscope near the focal plane, we measured the beam position while sequentially scanning a narrow pair of *xy* slits through the beam in a position close to the upstream side of the first mirror. Motion of the apparent beam spot on the YAG reveals slope errors in each isolated part of the mirror. (The beam would stand still if all parts of the mirror were focused to the same position.) These tests were performed first on the upstream mirror alone, and then with the second mirror in position, in order to separate any correlated effects. This technique is effective for getting the two mirror foci to coincide on the same focal plane. Also, the (anticipated) highly

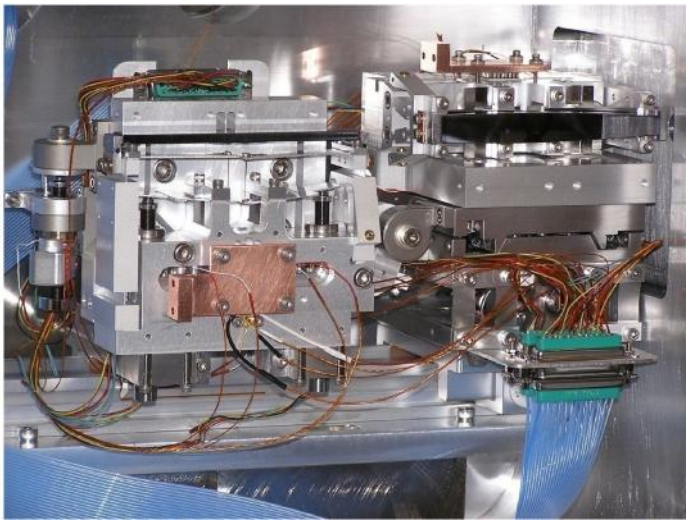

Figure 6: An orthogonal pair of temperature-controlled, in-vacuum KB mirror mounts for ~100-mm-long mirror substrates. The mounts, which share an optical rail, have five degrees of freedom (upstream and downstream bending plus height, tilt, and roll), and a Peltier cooler that attaches to a heat sink.

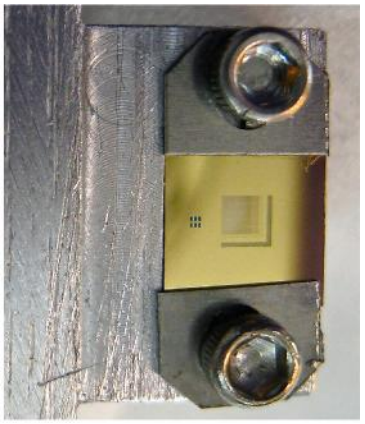

Figure 7: Nanofabricated optical elements, including knife-edges, slits, and gratings, are patterned in a compact design on a 2 x 2 mm silicon-nitride window in a small silicon chip. The patterns are etched in a 1-µm-thick gold layer, and the chip is mounted to an xyz stage positioned near the focal plane.

degenerate coupling of the mirror tilt angle and bending was observed. At low angles of incidence, changes to the glancing angle (from mirror tilting) steer the beam laterally, and change the focal distance dramatically. The axis of the tilting mechanism is centered on the center of the mirror surface to avoid motion of the beam footprint and undesirable beam displacements.

4. **A scanning Hartmann test.** A dense array of patterns for optical metrology (described later) was nanofabricated onto a gold absorber layer on a 2 x 2 mm silicon-nitride window (Figure 7). The supporting silicon wafer chip was mounted to a *xyz* stage near the KB focus, held perpendicular to the beam's central ray. The pattern contains a second pair of *x* and *y* slits with 10 gm openings. The beam is scanned in a plane downstream of focus and the projected spot is observed on the far-away CCD camera, in a configuration analogous to a Hartmann test [27, 28] made with sequential steps.
5. **Knife-edge test.** In what is commonly called the Foucault test [29], the array's *x* and *y* knife edges are scanned through the beam near focus. Either the CCD or a photodiode can be used to measure the transmitted light intensity past the knife-edge. The signal measured as the edge scans across the focus is the one-sided integral of the beam profile up to the knife position, and its derivative reveals the beam shape and width. Compared to other methods, this knife-edge test is straightforward and difficult to misinterpret, and it senses the beam in focus where our interest lies. The downside is that, without some degree of automation and rapid collection, the test can be time-consuming, and it requires a search through multiple *z* planes to find best focus. Furthermore, since each measurement point is collected independently, the test is vulnerable to any kind of vibration, instability, intensity variation, or knife position errors.
6. **Shearing interferometry.** Perhaps the most versatile test investigated in this project is grating-based shearing interferometry [30]. Shearing enables the simultaneous measurement of the *x* and *y* gradients of the wavefront. More accurately, shearing provides a result closely related to the discrete derivative. Here, a single 1D or 2D grating is placed in the diverging beam just downstream of focus, and the grating pattern is projected onto the CCD camera. Choosing a relatively coarse grating creates a small diffraction angle relative to the beam cone, providing a high degree of beam overlap (above 90%) in the detector plane. The overlap may be viewed as the interference of multiple displaced copies of the test wavefront.

For high-contrast fringes, the longitudinal (*z*) position of the grating is important, due to the Talbot effect for diverging beams. With the detector far from focus, the grating positions for highest contrast are approximately given by $z_n = nd^2$IX. The first-order (n = 1) positions for wavelength X = 1 nm and grating pitch d = {4, 5, and 6 gm} are {16, 25, and 36 mm} from focus. In practice the *z* position tolerance is greater than 1 mm in this configuration. In line with the expectations of Talbot self-focusing, the intensity fringes observed in these shearing interferograms are sharp and square, like the grating used to produce them. Figure 8 shows a series of 1D shearing interferogram details created by moving the 5-µm-pitch grating away from focus in 1 mm

steps.

Shearing interferograms recorded during mirror alignment are shown in Figure 9. The rectangular pupil results from different numerical aperture values in the two directions (2.7 and 1.3 mrad, respectively). Dust and imperfections on the mirror surfaces cause the dim patches in the interferograms.

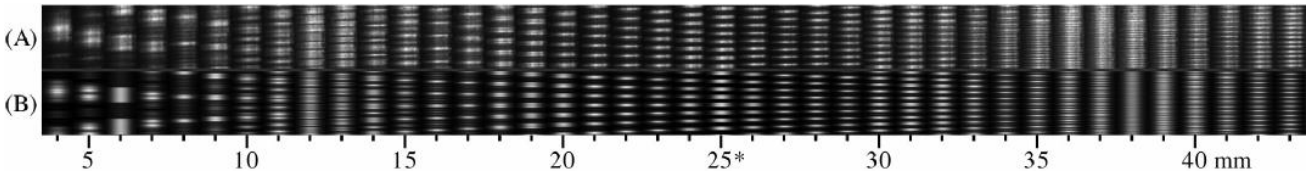

Figure 8: (A) Measured and (B) predicted 1D shearing interferogram details recorded as the 5-µm-pitch grating moves away from focus in 1 mm steps. With 1-nm wavelength, the peak contrast Talbot plane is anticipated to be close to 25-mm. Comparison with theory reveals a wavelength miscalibration of a few percent.

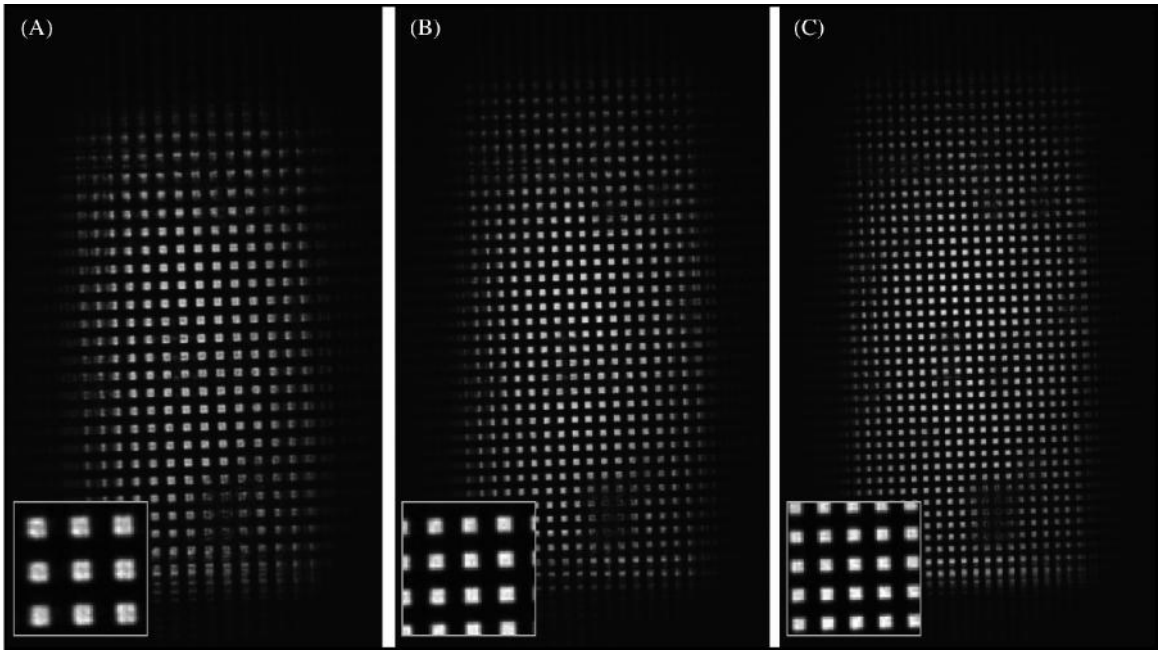

Figure 9: A sequence of three, two-dimensional shearing interferograms recorded with cross-grating pitches of (A) 4 µm, (B) 5 µm, (C) 6 µm, in the first Talbot plane of each. The inset details are extracted from the centers of each interferogram.

In practice, shearing requires several mathematical steps to analyze and recover the incident wavefront, but the results can also be easily interpreted by eye. When one of the KB mirrors was not orthogonal to the other, we observed tilted, non-perpendicular fringes. Furthermore, changes in the fringe pitch across the pupil show clear evidence of coma and higher aberrations. A difference in pitch between the overlapping *x* and *y* patterns is evidence of astigmatism.

A significant advantage of shearing, similar to the Hartmann test, is that a single recorded interferogram can reveal the instantaneous state of the system—no scanning is required—and the analysis can be performed in under a second. To improve the signal-to-noise ratio and the spatial frequency response, a short phase-shifting series can be recorded by moving the grating in a series of lateral steps and adding an additional step to the analysis.

The speed of the shearing measurements enable feedback and alignment to proceed on short timescales. We used shearing to determine the wavefront sensitivity to each degree of freedom (benders, tilt, and position actuators.) Once the error dependencies are known, various techniques, including the method of characteristic functions (see, e.g., [3, 4] and references therein) and singular-value decomposition, can be used to optimize the system alignment.

Generally speaking, in experiments where the beam is projected onto a camera behind the sample plane (such as coherent diffraction imaging) or where there is room for a camera behind a sample, a shearing system could be incorporated to provide feedback for adaptive control or manual adjustment.

For loop-closing comparisons with optical metrology, it is important not to neglect the nonlinear coordinate transformation that projects positions in the measured wavefront slope back onto the curved surfaces of the test mirrors. That transformation must be evaluated for each unique configuration. Furthermore, varying distances between points on the mirror surface and the focal plane lead to a position-dependent variation in the sensitivity to local slope errors. The farther the mirror is from focus, the greater the sensitivity to slope errors will be.

Reflectometry: An always-reliable bank shot

Reflectometry is one of the most flexible and frequently used tools in the short-wavelength metrology toolkit. Having a reliable and accurate measurement system for reflected and transmitted light of calibrated wavelengths sets the stage for fundamental studies of the optical properties of bulk and thin-film materials, compounds, coatings, multi-layers, and other structured matter used in X-ray optics.

The successful design and engineering of simple to complex optical elements and systems relies foremost on a basic knowledge of the materials' properties. Reflectometry is used on both surrogates and completed parts to test the efficiency of coatings, to quantify scattering magnitudes, and as feedback to support the development of coating recipes for specialized components.

The ALS Reflectometer for Calibrations and Scattering, on beam- line 6.3.2, has been in operation since 1994, serving to improve the quality of countless beamlines and optical systems operating in the wavelength range of 1 to 50 nm (25-1300 eV).

One of the most promising avenues for improved resolution at existing and future beamlines comes from major advances in the line density of spectrometer or monochromator gratings. For example, the reflectometer has been used to verify 25% first-order efficiency from 10,000 line/ mm, multilayer-coated gratings fabricated on anisotropically etched Si substrates [23], providing feedback for grating nanofabrication.

Demand from the EUV photolithography community, in the semiconductor chip-making industry, is pushing reflectometry tools to accommodate optics with ever-larger diameters. Certain aspherical mirrors in compound-element EUV imaging lenses exceed the width of a serving platter, with thicknesses of many inches and masses of tens of kilograms. These marvels of optical fabrication now meet diffraction-limited specifications for their design wavelength, near 13.5 nm. They have surface figure quality levels below 0.5 nm (rms), and mid-and high-spatial frequency roughness to match.

Recent upgrades to the ALS Reflectometer enable it to now accept optics up to 300 mm and 15 kg. The stages and controls enable the detectors to follow the reflected beam path across the curved surfaces, and measure the reflectivity to within 0.1%.

Since the power lost to scattering is typically proportional to X^{-4}, short wavelength optics have *much* tighter surface roughness specifications than their visible-light counterparts. Complicating advancement is the fact that as the fabrication of smooth optical surfaces has improved, optical characterization tools are reaching their practical limits for roughness detection. Short-wavelength scattering measurements from the reflectometer are now used to benchmark optical tools, extending their useful capabilities, and allowing manufacturers to have greater predictive power in the optics shop.

Nanofabrication: Making the point for diffractive optical structures in metrology

From the first days of operation at the ALS, in the mid-1990s, nano-fabricated optical elements, including diffraction gratings, pinholes, and specialized structures, have served as calibrated reference objects in beam-focusing metrology.

The use of electron-beam lithography in the fabrication of Fresnel zoneplate lenses is a well-known example of where progress in the creation of fine, free-form structures approaching 10-nm linewidths has led to progress in nanoscale imaging microscopy [28]. Fresnel zoneplates are holographic lenses that operate by diffraction rather than refraction or reflection, making them suitable for short wavelengths where high-quality lenses are otherwise unavailable or prohibitively expensive.

Less well-known, perhaps, is the application of the same fabrication techniques to make calibrated structures for interferometry, pinhole spatial filters, knife edges, and other reference patterns that aid metrology. Relatively opaque materials such as gold and nickel support robust, binary patterns, with EUV and soft X-ray wavelength-scale feature sizes and high-aspect ratios (i.e., thick with narrow grooves) when required. The Nanowriter electron-beam lithography tool at LBNL’s Center for X-ray Optics has specialized control hardware for generating curved shapes at high resolutions [29]. These optics can be created on thin

membranes, such as silicon-nitride, or as free-standing, stencil-type patterns for higher efficiency.

Recent examples of structures created specifically for metrology include: (a) a compound focal-plane metrology pattern used for KB mirror testing [26]; (b) pinholes for generating spherical wavefronts; and (c) binary pseudo-random (BPR) patterns [17] (described above) used to provide detailed characterizations of the resolution of optical and X-ray microscopes.

Conveniently, several metrology techniques for testing short-wave-length focusing optics rely on similar hardware configurations. In the knife-edge test, the scanning-slit test, and grating-based shearing interferometry, a nanofabricated optical element (shown in Figure 7) is placed in the vicinity of the focal plane, and the transmitted light is captured downstream either by a photodiode or a CCD camera. The test structures used in the KB mirror experiments described above are integrated into a single, compound optical element on a 2 x 2 mm widow silicon-nitride window. A 1-gm absorber thickness provides 99.8% absorption at 1-nm wavelength.

In this structure, two orthogonal knife-edges are available for *x* and *y* beam-width measurements. A pair of narrow *x* and *y* slits are for beam profile and local wavefront slope measurements. Occupying most of the space are 1D gratings for isolated-KB-mirror measurements and 2D cross-gratings for full wavefront characterization. Various grating pitch values create a range of available shear magnitudes. Since the grating diffraction creates the split beams that interfere at the detector plane yielding the measurement, the grating line placement accuracy couples directly into the measured beam quality.

Pinhole spatial filters play an important role in testing optical systems with finite conjugate positions, like a KB mirrors. Pinholes, for spherical wavefronts, and slits for cylindrical wavefronts, are placed in the upstream conjugate position where they filter the aberrations from the beamline, and isolate the wavefront-error contributions imparted by imperfections and misalignments of the focusing optics. A beam diffracted from a slit or pinhole must be broad enough to fill the pupil of the lens under test, with some overfilling, if possible, to improve the quality of the wavefront across the relevant solid angle. Lithographically fabricated pinholes at or below 1-µm diameter in several-micron-thick absorber layers have shown excellent performance, blocking transmitted light, filtering the aberrations of the beamline upstream of the optics under test, generating spatial coherence required for interferometric tests, and providing a stable point source for wavefront measurement.

In ongoing work, the Nanowriter has also been used to fabricate structures for beamline spatial-coherence testing, using pinhole arrays to mimic many sets of Young-type double-slit experiments in parallel.

Conclusion

In its many forms, metrology data is the essential feedback that enables progress in short-wavelength nanoscience. The demands on metrology are continually increasing. We have reviewed the X-ray optics metrology network developed at the ALS, which includes a set of ex-situ metrological tools in the ALS X-ray Optics Laboratory, an at-wavelength metrology test set up at the ALS BL 5.3.1, the ALS Reflectometer for Calibrations and Scattering on beamline 6.3.2, and the CXRO Nanowriter electron-beam lithography tool, working together with shared goals. These complementary metrology tools and the collective expertise that guides their use are essential for ensuring high-performance and continued scientific productivity of the ALS beamlines. Where improved metrology tools can be used offline or incorporated directly into beamlines, the scientific programs will benefit. The ongoing dialog and rich collaborations that have developed among metrologists at laboratories worldwide seed the ground for another generation of progress.

Acknowledgements

The authors are very grateful to Samuel Barber, Kenneth Chow, Raymond Conley, Curtis Cummings, Edward Domning, Ralf Geckeler, Nicholas Kelez, Jonathan Kirschman, James Macdougall, Elizabeth Martin, Iacopo Mochi, Gregory Morrison, Simon Morton, Patrick Naulleau, Tino Noll, Frank Siewert, Brian Smith, Peter Takacs, Jeffrey Takakuwa, Tony Warwick, Anthony Young, Sam Yuan, and Thomas Zeschke for extremely productive and enjoyable collaboration on development and application of metrology for X-ray optics at the ALS. The Advanced Light Source is supported by the Director, Office of Science, Office of Basic Energy Sciences, Material Science Division, of the U.S. Department of Energy under Contract No. DE-AC02-05CH11231 at Lawrence Berkeley National Laboratory. This work was supported by the Laboratory Directed Research and Development Program of Lawrence Berkeley National Laboratory.

References

1. J. L. Kirschman et al., *Proc. SPIE* **7077**, 70770A-1-12 (2008).
2. V. V. Yashchuk et al., *Nucl. Instrum. and Methods A* **616**(2–3), 212–223 (2010).
3. W. R. McKinney et al., *Opt. Eng*. **48**(8), 083601-1-8 (2009).
4. W. R. McKinney et al., *Proc. SPIE* **8141**, 81410K-1-14 (2011).

5. V. V. Yashchuk et al., *Journal of Physics: Conf. Ser.* **425**, 152003 (2013).
6. F. Siewert, H. Lammert, T. Zeschke, *Modern Developments in X-ray and Neutron Optics*, Springer, Berlin (2008).
7. S. G. Alcock et al., *Nucl. Instrum. and Methods A* **616**(2-3), 224-228 (2010).
8. J. Nicolas and J. C. Martinez, *Nucl. Instr. and Meth. A* **710**, 24-30 (2013).
9. Y. Senba et al., *Nucl. Instrum. and Methods A* **616**(2-3), 237-240 (2010).
10. V. V. Yashchuk, *Rev. Sci. Instrum.* **80**, 115101-10 (2009).
11. Z. Ali et al., *Proc. SPIE* **8122**, 8141-23 (2011).
12. V. V. Yashchuk et al., *Proc. SPIE* **6704**, 67040A (2007).
13. S. Yuan et al., *X-ray Optics and Instrumentation* **2010**, 784732/1-9 (2010).
14. V. V. Yashchuk, W. R. McKinney, and N. A. Artemiev, *Nucl. Instr. and Meth. A* **710**, 59-66 (2013).
15. Y. V. Yashchuk and V. V. Yashchuk, *Opt. Eng.* **51**(4), 046501 (2012).
16. V. V. Yashchuk, W. R. McKinney, and P. Z. Takacs, *Opt. Eng*. **47**(7), 073602-1-5 (2008).
17. S. K. Barber et al., *Nucl. Instr. and Meth. A* **616**, 172-182 (2010).
18. V. V. Yashchuk et al., *Opt. Eng.* **50**(9), 093604 (2011).
19. V. V. Yashchuk et al., *Nucl. Instr. and Meth. A* **649**(1), 150-152 (2011).
20. S. K. Barber et al., *Opt. Eng.* **49**(5), 053606/1-9 (2010).
21. D. L. Voronov et al., *Opt. Lett.* **35**(15), 2615-8 (2010).
22. D. L. Voronov et al., *J. Appl. Phys.* **111**(9), 093521-1-9 (2012).
23. D. L. Voronov et al., *Opt. Lett.* **37**(10), 1628-1630 (2012).
24. D. L. Voronov et al., *Journal of Physics: Conf. Ser.* **425**, 152006 (2013).
25. D. J. Merthe et al., *Proc. SPIE* **8139**, 813907-1-17 (2011).
26. D. J. Merthe et al., *Opt. Eng.* **52**(3), 033603-1-13 (2013).
27. Hartmann X-ray beam metrology and X-ray optic alignment by Hartmann wavefront sensing.
28. P. Mercère et al., *Optics Letters* **31**(2), 199-201 (2006).
29. E. Gaviola, *J. Opt. Soc. Am*. **26**, 163-169 (1936).
30. P. P. Naulleau, K. A. Goldberg and J. Bokor, *Journal of Vacuum Science and Technology B* **18**(6), 2939-43 (2000).
31. S. Yuan et al., *Nuclear Instruments and Methods in Physics Research A* **635**, S58-S63 (2011).
32. W. Chao et al., *Optics Express* **20**(9), 9777-9783 (2012).
33. E. H. Anderson et al., *J. Vac. Sci. Technol. B* **18**(6), 2970-2975 (2000).

DISCLAIMER